Supplementary Information

This PDF file includes:

1. Legends for Supporting Videos 1 to 3
2. Supporting Figures S1 to S7
3. Discussion Part for Adhesion
4. Coulomb Friction Model Validation through Friction Experiment

1. Legends for Supporting Videos

Supporting Video 1: Exp1.mp4. Video of the experiment of PDMS pillars with $\Delta x = 0$, $H_c = 2.8\ mm$ for $2R = 3\ mm$, and height $L = 4.8\ mm$ (sliding velocity: 0.05 mm/s).

Supporting Video 2: FE1.mp4. Video of the motion of PDMS pillars with $\Delta x = 0$, $H_c = 2.8\ mm$ for $2R = 3\ mm$, and height $L = 4.8\ mm$ (sliding velocity: 0.2 mm/s).

Supporting Video 3: FEcontact.mp4. Video of the motion of two pieces of PDMS pillars with $\Delta x = 0$, $H_c = 2.8\ mm$ for $2R = 3\ mm$, and height $L = 4.8\ mm$ (sliding velocity: 0.2 mm/s).

2. Convergence Tests for FE simulation

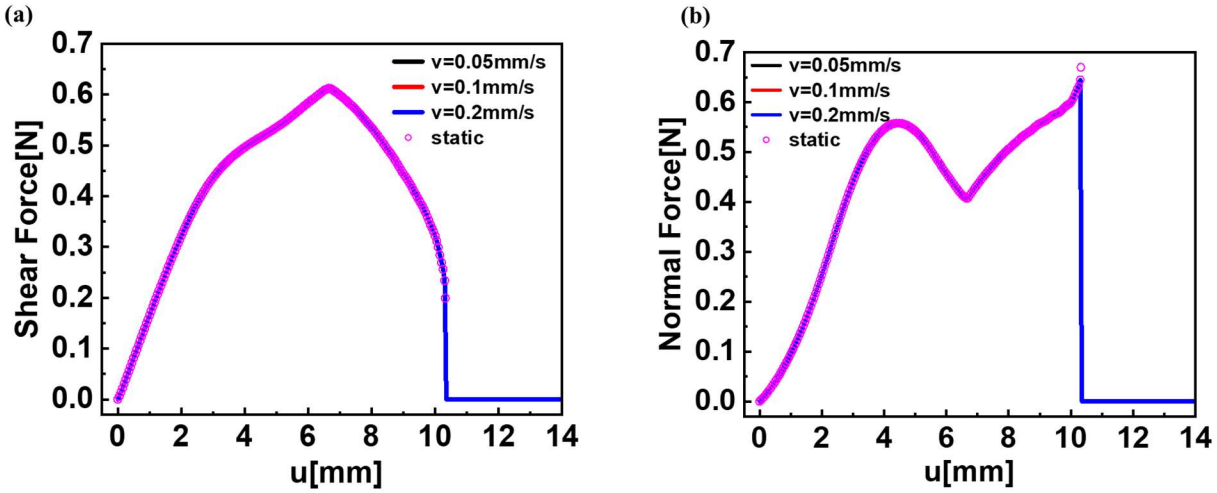

Figure S1. Velocity convergence test and solver convergence test for FE simulation cases with $2R = 3\ mm$, $L = 4.8\ mm$, $\Delta x = 0$, $H_c = 2.8\ mm$, $\mu = 0.4$. (a) Shear force versus horizontal displacement u, (b) Normal force versus horizontal displacement u for different velocities in DIQ solver and static solver.

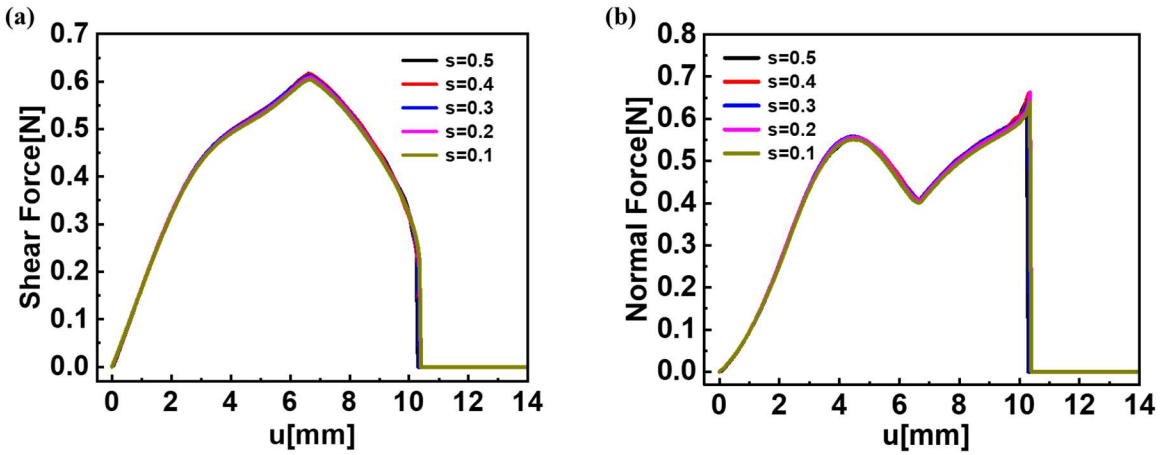

Figure S2. Mesh convergence tests for FE simulation cases with $2R = 3\ mm$, $L = 4.8\ mm$, $\Delta x = 0$, $H_c = 2.8\ mm$, $\mu = 0.4$. s is the mesh size with unit [mm]. The pillar is meshed uniformly by $s\ mm \times s\ mm \times s\ mm$. Element size in substrate gradually increases from $s\ mm \times s\ mm \times 1\ mm$ near the pillar to the $1\ mm \times 1\ mm \times 1\ mm$ at the edges. (a) Shear force versus horizontal displacement u for different mesh sizes. (b) Normal force versus horizontal displacement u for different mesh sizes.

3. FE simulation results with constant friction coefficient $\mu = 0.4$ for two lateral overlaps, $l_x = 0.75$, $l_x = 0.5$

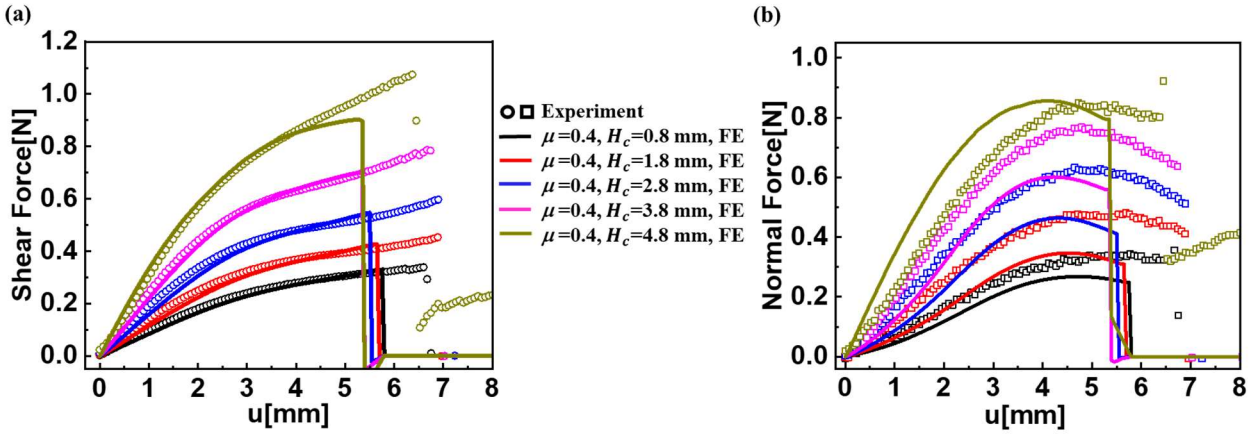

Figure S3. FE simulation results (solid lines) ($\mu = 0.4$) & experimental results (symbols) for 5 different heights of contact H_c with $2R = 3\ mm$, $L = 4.8\ mm$, $l_x = 0.75$. (a) Shear force versus horizontal displacement u. (b) Normal force versus u.

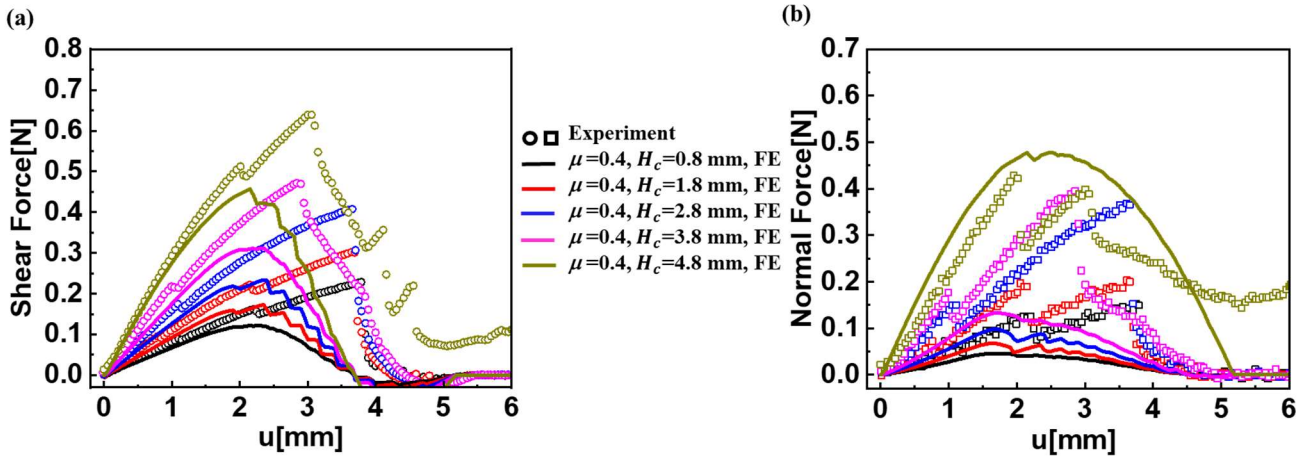

Figure S4. FE simulation results (solid lines) ($\mu = 0.4$) & experimental results (symbols) for 5 different heights of contact H_c with $l_x = 0.5$. (a) Shear force versus horizontal displacement u. (b) Normal force versus u.

4. The FE simulation results for pillars with diameter $2R = 3\ mm$, and height $L = 6\ mm$

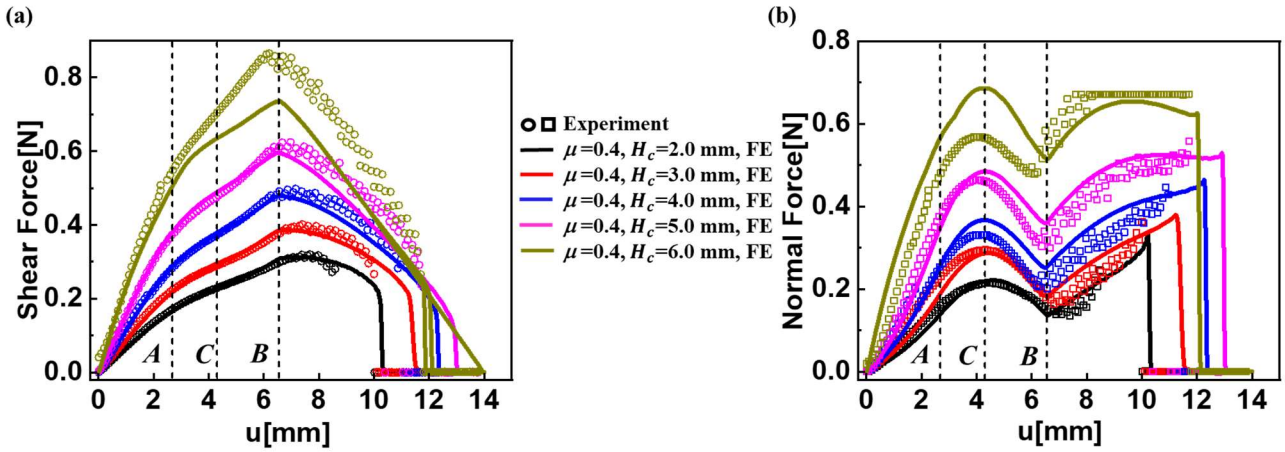

Figure S5. FE simulation results (solid lines) ($\mu = 0.4$) & experimental results (symbols) for 5 different heights of contact H_c with $l_x = 1$ (no lateral offset), $L = 6\ mm$ and $2R = 3\ mm$. (a) Shear force versus horizontal displacement u. (b) Normal force versus u. Before point A, the pillars are sliding relatively. Between A and B, there is no global sliding between the two pillars. After point B, the pillars are sliding relatively again. The normal force arrives at its first peak at point C.

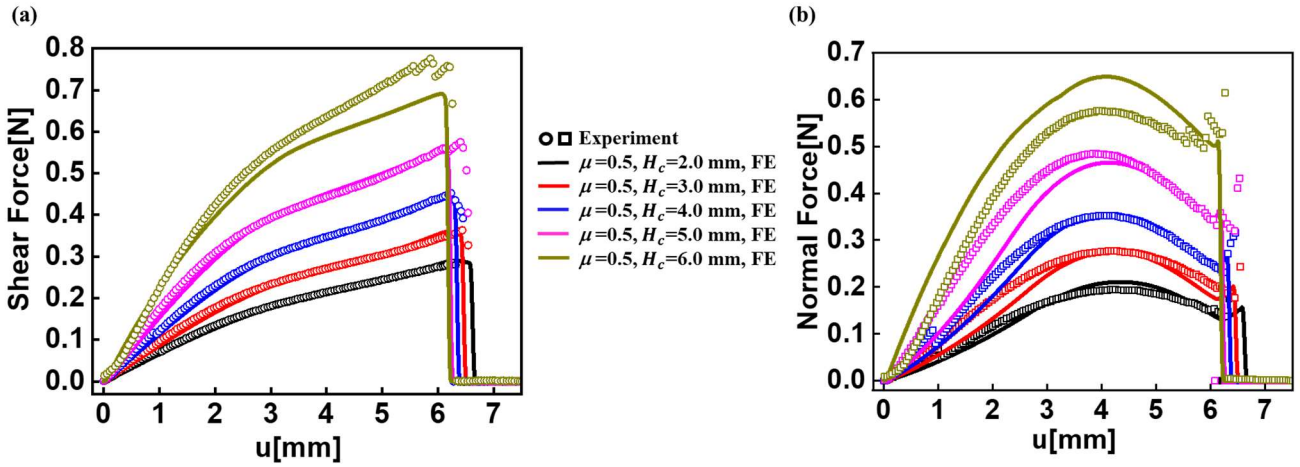

Figure S6. FE simulation results (solid lines) ($\mu = 0.5$) & experimental results (symbols) for 5 different heights of contact H_c with $l_x = 0.75$, $L = 6\,mm$ and $2R = 3\,mm$. (a) Shear force versus horizontal displacement u. (b) Normal force versus u.

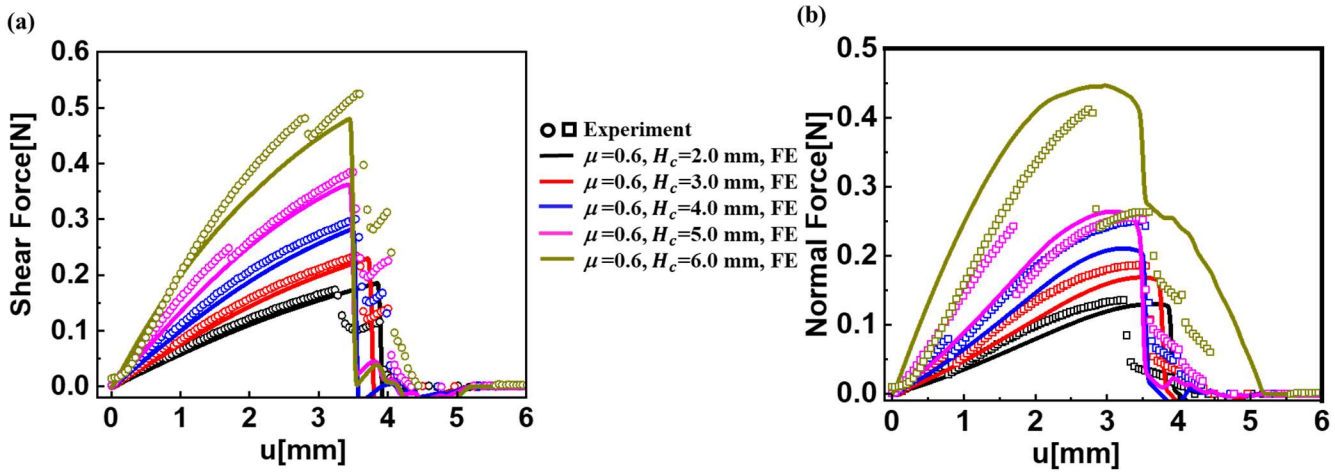

Figure S7. FE simulation results (solid lines) ($\mu = 0.6$) & experimental results (symbols) for 5 different heights of contact H_c with $l_x = 0.5$, $L = 6\,mm$ and $2R = 3\,mm$. (a) Shear force versus horizontal displacement u. (b) Normal force versus u.

5. Discussion

Adhesionless contact of a rigid sphere in contact with an incompressible elastic substrate – Hertz theory:

The pressure distribution $p(r)$ inside the contact circle of radius a can be found in Johnson [1], i.e.,

$$p(r<a) = \frac{8Ga}{\pi R}\left(1-\frac{r^2}{a^2}\right)^{1/2} \qquad \text{where } a = \left(\frac{3RN}{16G}\right)^{1/3}, \qquad \text{S1}$$

where R is the radius of the sphere, G is the shear modulus of substrate and r is the radial distance from the center of the contact circle. The shear force S that is needed to initiate sliding is estimated by evaluating the integral

$$S = 2\pi\int_0^a \mu p(r) r dr = 2\pi\mu\int_0^a p(r) r dr = \mu N \ . \qquad \text{S2}$$

The last identity is due to force balance and a constant friction coefficient.

JKR theory for the case of N = 0

The contact radius at any normal load N is given by Johnson [1]

$$\left(N - \frac{16Ga^3}{3R}\right)^2 = 32\pi W_{ad} G a^3, \qquad \text{S3}$$

where we have specialized Johnson's expression for an incompressible elastic substrate in contact with a rigid sphere. The contact radius a_0 given by Eq. (2) is obtained by setting N = 0 in S3. The pressure distribution is [1]

$$p(r<a) = \frac{8Ga}{\pi R}\left(1 - \frac{r^2}{a^2}\right)^{1/2} - \sqrt{\frac{8GW_{ad}}{\pi a}}\left(1 - \frac{r^2}{a^2}\right)^{-1/2}. \qquad \text{S4}$$

The first term in S4 is compressive while the 2nd term is tensile. For N = 0, $a = a_0$, the radius c where compression is greater than or equal to the tension is obtained by setting $p = 0$ in S4 and solve for the root, which results in

$$1 - \frac{c^2}{{a_0}^2} = \sqrt{\frac{8GW_{ad}}{\pi a_0}}\frac{\pi R}{8Ga_0} = \frac{1}{3} \Rightarrow \frac{c^2}{{a_0}^2} = 2/3 \ , \qquad \text{S5}$$

where in the last step, we have used (1). The shear force S based on Coulomb model is obtained by integrating S4 over the circle $r < c$, where only compressive stress acts, i.e.,

$$S = 2\pi\mu\int_0^c \left[\frac{8Ga_0}{\pi R}\left(1 - \frac{r^2}{a_0^2}\right)^{1/2} - \sqrt{\frac{8GW_{ad}}{\pi a_0}}\left(1 - \frac{r^2}{a_0^2}\right)^{-1/2}\right] r dr = \mu\frac{16Ga_0}{R}\int_0^c \left[\left(1 - \frac{r^2}{a_0^2}\right)^{1/2} - \frac{1}{3}\left(1 - \frac{r^2}{a_0^2}\right)^{-1/2}\right] r dr$$

S6

In the 2nd step, we used S5. The integral in the last equation of S6 can be evaluated exactly, and S is given by

$$S = \frac{4\pi\mu W_{ad} R}{\sqrt{3}} \ . \qquad \text{S7}$$

6. Pillar-Pillar Sliding Experiment

To validate the Coulomb friction model utilized for PDMS-PDMS contact, we performed friction experiments involving two cylindrical pillars (refer to Figure S8). The fabrication process for these pillars followed the methodology outlined in Section 2.1 of the Methods and Materials. Both pillars have a diameter of 3 mm, but differ in height: one measures 4.8 mm, while the other stands at 30 mm (see Fig.S8).

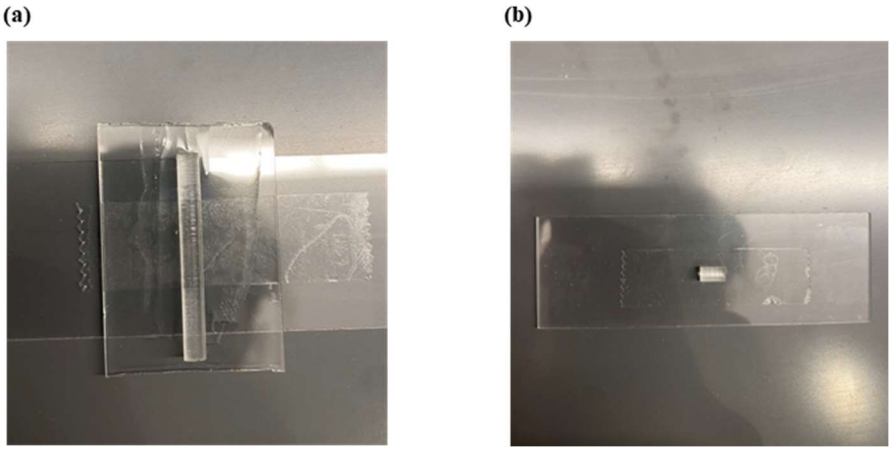

Figure S8. Cylindrical fibers. (a) Cylindrical pillar with length ~30 mm. (should be long enough to perform sliding experiment) (b) Cylindrical pillar with diameter 3mm and length 4.8 mm.

During the experiment, the two cylinders were affixed to glass slides using PDMS (10:1 ratio by mass) as an adhesive between the pillars and the glass surface. These cylinders were positioned perpendicular to each other, with the shorter pillar being fixed (refer to Fig. S9).

Initially, the pillars were brought into contact by vertically displacing them, and the resulting normal and shear forces were recorded in a text file. Once a slight contact was established, indicated by the presence of a normal force, we initiated shear displacement on the longer cylinder at a rate of 0.01 mm/s, covering a distance of 6 mm. Once the shear force reached a stable value (around 0.5 mm of sliding), we gradually increased the vertical load by incrementally raising the vertical displacement at a rate of 0.001 mm/s. This meant that for every 600 seconds of shear sliding, the vertical displacement increased by 0.6 mm. The shear force was recorded as the normal load increased.

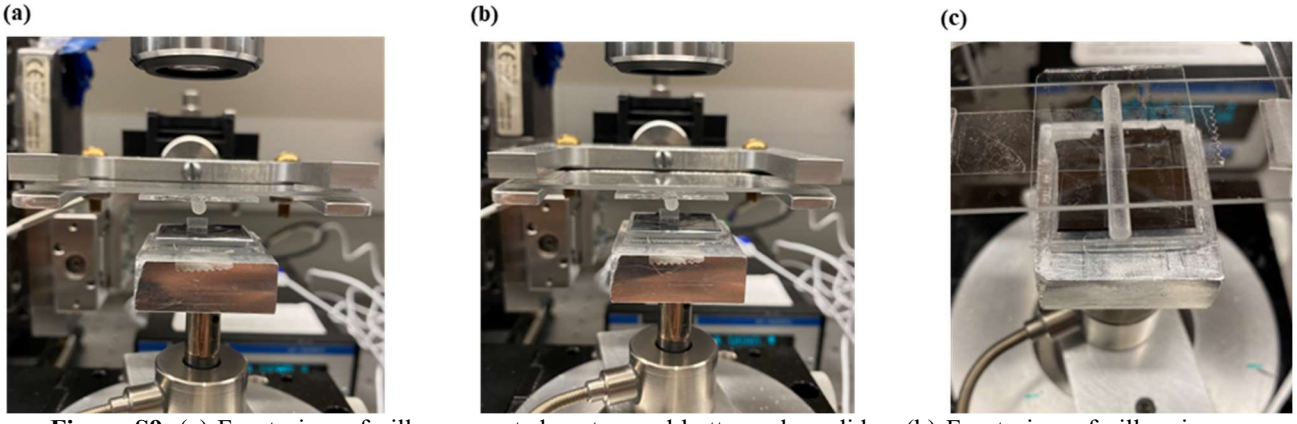

Figure S9. (a) Front view of pillars mounted on top and bottom glass slides. (b) Front view of pillars in contact. (c) Top view of pillars mounted on the setup.

The data obtained for shear force, normal force, and sliding displacement were plotted (Figure S10), allowing us to calculate the coefficient of friction (μ) as the ratio of shear force to normal force. Based on Figure S10 (c), we observed that the ratio gradually stabilized at a constant value, which confirmed the validity of the phenomenological Coulomb friction model.

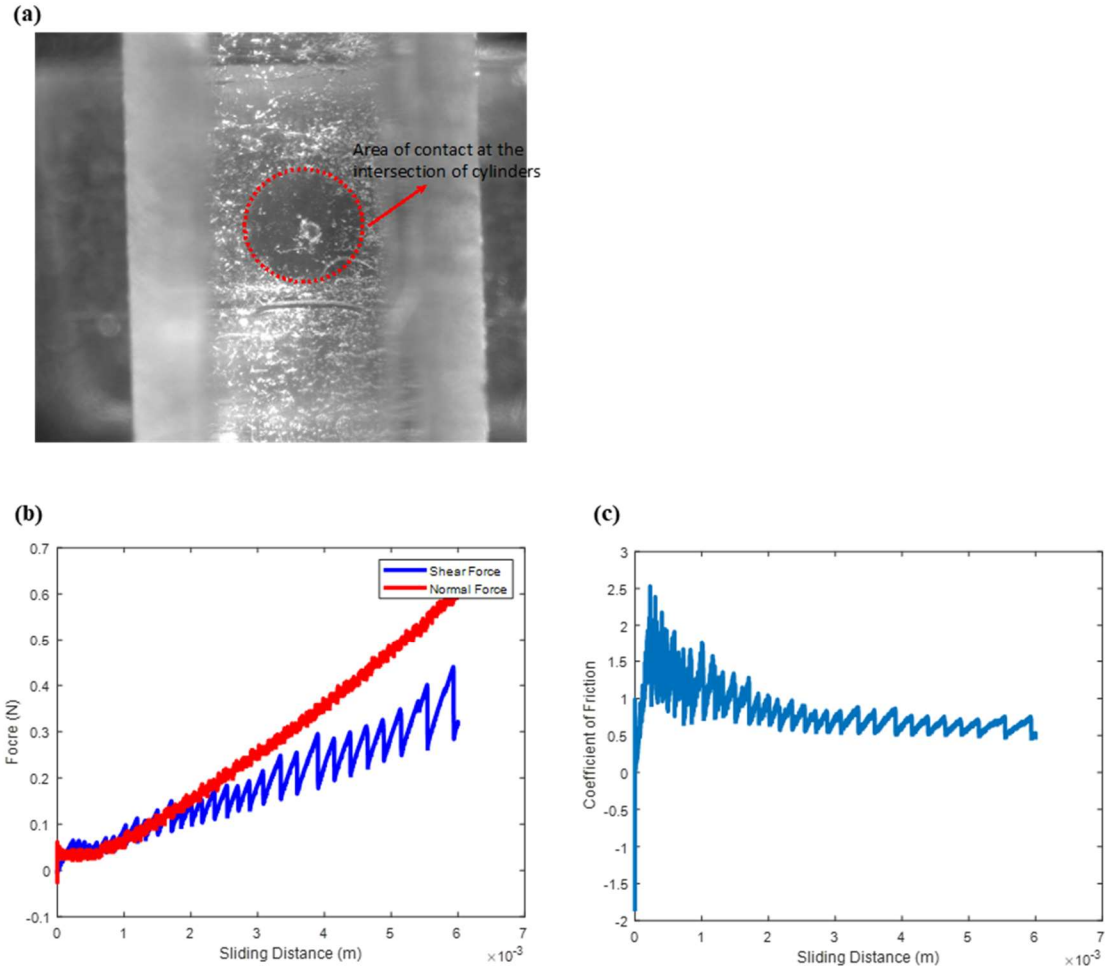

Figure S10. (a) A visualization of the cylindrical pillars in contact, showing the circular contact area at the interface. (b) Shear and Normal Force versus displacement for friction experiment. (c) Variation of coefficient of friction with sliding displacement.

Reference

1 K. L. Johnson and K. L. Johnson, *Contact Mechanics*, Cambridge University Press, 1987.